PAPER

Influence of temperature and pressure on cumulants and thermodynamic parameters of intermetallic alloy based on anharmonic correlated Einstein model in EXAFS

IOP Publishing Physica Scripta
Phys. Scr. 95 (2020) 075706 (7pp) https://doi.org/10.1088/1402-4896/ab90bf

Influence of temperature and pressure on cumulants and thermodynamic parameters of intermetallic alloy based on anharmonic correlated Einstein model in EXAFS

Nguyen Ba Duc

Faculty of Physics, Tan Trao University, Tuyen Quang, Vietnam

E-mail: ducnb@daihoctantrao.edu.vn

Received 15 March 2020, revised 29 April 2020
Accepted for publication 6 May 2020
Published 14 May 2020

Abstract

The extended x-ray absorption fine structure (EXAFS) spectroscopy is one of the powerful techniques for investigating local structures of crystalline as well as amorphous materials. It provides different structural information at various high temperatures due to anharmonicity. This work advances the anharmonic correlated Einstein model in EXAFS to investigate how pressure and temperature affect the Debye-Waller factor and thermodynamic parameters of an intermetallic alloy. By using the anharmonic correlated Einstein model, analytical expressions derived include the effective elastic constants, the EXAFS cumulants, the anharmonic factor, and the thermal expansion coefficient under high temperature and pressure effect. The results show that the anharmonicity of the thermal atomic vibration and the consequences of pressure are both essential for the thermodynamic parameters and the EXAFS Debye-Waller factor, as well as showing that the anharmonic contributions are necessary for the EXAFS spectrum. Numerical calculations of these thermodynamic quantities performed for pure Cu and Ag and CuAg72 alloy and the results are consistent with those obtained experimentally and from other theories.

Keywords: anharmonic, cumulant, Debye–Waller factor, intermetallic alloy, pressure

(Some figures may appear in colour only in the online journal)

1. Introduction

Extended x-ray absorption fine structure (EXAFS) spectroscopy has developed into a powerful probe of atomic structure and the high-temperature thermodynamics of substances due to anharmonicity [1, 2]. The formalism for including anharmonic effects in EXAFS often written based on the cumulant expansion approach. Many methods have developed to study the temperature dependence of EXAFS cumulants. However, to the best of our knowledge, no theoretical calculations have been done to predict the relationship of cumulants and thermodynamic parameters on temperature with effects of pressure in EXAFS spectra of cubic crystals. It requires a more accurate interatomic interaction form for metallic systems, such as the many-body embedded-atom potentials.

Numerous methods have evolved to investigate how temperature affects the EXAFS cumulants, such as path-integral effective-potential theory [3], the statistical moment method [4], the ratio method [5], the Debye model [6], the Einstein model [7], and the anharmonic correlated Einstein model (ACEM) [8]. Several groups have applied ACEM theory to EXAFS to study how the thermodynamic properties depend on temperature with the effect of the material doping ratio [9–12]. However, no reports to date have discussed how the thermodynamic parameters and the Debye–Waller factor (DWF) depend on temperature and pressure for Cu, Ag, and their intermetallic alloy CuAg72. A CuAg alloy contains the elements Cu and Ag, with the Ag atoms referred to as the substitution atoms and the Cu atoms referred to as the host atoms. CuAg72 has a ratio of 72% Ag and 28% Cu (±1%) and is also known as *CuSil* or *UNS P0772* (note: *CuSil* should

not be confused with *Cusil-ABA*, which has the composition 63.0% Ag, 35.25% Cu, and 1.75% Ti). It is a eutectic alloy and is used primarily for vacuum brazing [9].

Herein, we use EXAFS theory [8] to investigate how the DWF depends on the temperature at high pressure. We also investigate thermodynamic parameters such as (i) the effective spring constant, (ii) the thermal expansion coefficient, (iii) the anharmonic factor, and (iv) the Einstein frequency and temperature and how they depend on the temperature at ambient pressure for CuAg72.

2. Formalism

EXAFS usually derived by using the cumulant-expansion approach, which contains the second cumulant σ^2 corresponding to the parallel mean-square relative displacement (MSRD) [5]. The second cumulant - often called the DWF - is an important factor in EXAFS analysis because the thermal lattice vibrations and high pressure strongly influence the EXAFS amplitudes through the function $e^{-2\sigma^2 k^2}$ [1, 13]. For simplicity, the temperature and pressure dependences of the DWF are denoted as $\sigma^2(T)$ and $\sigma^2(p)$, respectively. One way to investigate how temperature and pressure affect the EXAFS cumulant is to combine ACEM with EXAFS [8, 14], which gives results that are consistent with experiments. ACEM uses the anharmonic effective interaction potential under pressure p, and the interatomic distance x is supplemented by $\delta r(p)$ to give

$$V_E(x, p) \approx \frac{1}{2}k_{eff}(x\delta r(p))^2 + k_{3eff}(x\delta r(p))^3 + k_{4eff}(x\delta r(p))^4..., \quad (1)$$

where k_{eff} is the effective spring constant, k_{3eff} and k_{4eff} are the effective cubic and quartic anharmonic parameters, respectively, which cause the asymmetry in the pair-distribution function, $\delta r(p) = r(p) - r(0)$ is the pressure-induced change in the interatomic distance, $x = r - r_0$ is the instantaneous bond length between atoms from the equilibrium location, r is the spontaneous bond length between absorbing and backscattering atoms, and r_0 is the equilibrium value of r. ACEM is determined by the vibration of single pairs of atoms, with M_1 and M_2 being the masses of the absorber and backscattering atoms, respectively. The oscillations of the absorber and backscattering atoms depend on their neighbors, so the interaction potential in equation (1) is written in the form of an anharmonic effective interaction potential under ambient pressure, namely

$$V_E(x, p) = V(x, p) + \sum_{i=1,2}\sum_{j\neq i} V\left(\frac{\mu}{M_i}x\delta r(p)\hat{R}_{12}\hat{R}_{.ij}\right). \quad (2)$$

In equation (2), V(x, p) is the interaction potential between absorbing and backscattering atoms, the sum i is over absorber (i = 1) and backscattering (i = 2) atoms, and the sum j is over all nearest neighbors whose contributions are described by the term V(x, p) excluding the absorber and backscattering atoms themselves. Furthermore, M_i is the atomic mass of atom i, μ is the reduced atomic mass, namely $\mu = M_1M_2/(M_1 + M_2)$, and $\hat{R}$ is the unit vector for the bond between atoms i and j. Therefore, this effective pair potential describes not only the interaction between absorber and backscattering atoms but also how the nearest-neighbor atoms affect such interactions, which is the difference between the effective potential used in this work and the single-pair potential [15] or single-bond potential [7], which consider only each pair of immediate-neighbor atoms [i.e., only V(x)] without considering the remaining terms on the right-hand side of equation (2). The atomic vibration is calculated using a quantum statistical approach with an approximate anharmonic vibration in which the system Hamiltonian includes a harmonic term H_0 with respect to the equilibrium at a given temperature plus an anharmonic perturbation, namely

$$H = H_0 + V_E(a) + \delta V_E(a). \quad (3)$$

Here, the interaction potential $V_E(a)$ and anharmonic perturbation $\delta V_E(a)$ are

$$V_E(a) = k_{eff}a^2/2 + k_{3eff}a^3,$$
$$\delta V_E(a) = (k_{eff} + 3k_{3eff}a^2)y + k_{3eff}y^2. \quad (3a)$$

where a is the thermal expansion coefficient with $a = \langle x\rangle$, $y = x - a$, $\langle y\rangle = 0$. Equation (3) leads to the ACEM interactive potential

$$V_E = V_E(a) + k_{eff}y^2 + \delta V_E(y), \quad (4)$$

which is an anharmonic potential of Morse pairs and is appropriate for approximating the structure of cubic crystals. The Morse anharmonic potential is

$$V(r) = D(e^{-2\alpha(r-r_0)} - 2e^{-\alpha(r-r_0)}) = D(e^{-2\alpha x} - 2e^{-\alpha x}), \quad (5)$$

where $D = -V(r_0)$ is the dissociation energy, so it has Electron-Volt (eV) unit, and α_{12} ($Å^{-1}$) is the width of the potential. We expand equation (5) in x to obtain the third-order term that describes approximately the cubic structure of doped crystals. When considering only crystals with orderly doping, we also assume that the lattice is not corrupted, and we designate Cu as the host atom with indicator 1 and Ag as the substituted atom with indicator 2. ACEM uses the Morse anharmonic pair potential to describe the pair interaction between atoms, namely

$$V_E(x, p) = D_{12}(e^{-2\alpha_{12}x\delta r(p)} - 2e^{-\alpha_{12}x\delta r(p)}) \approx D_{12}(-1 + \alpha_{12}^2(x\delta r(p))^2 - \alpha_{12}^3(x\delta r(p))^3 + ...). \quad (6)$$

For simplicity, we approximate the parameters of the Morse potential in equation (6) at a given temperature by $D_{12} = c_1D_1 + c_2D_2$, $\alpha_{12} = \sqrt{(D_1\alpha_1^2 + D_2\alpha_2^2)/(D_1 + D_2)}$, where c_1, c_2 are the doping ratios (%) of the intermetallic alloys. We calculate the sums in the second term of equation (2) and compare the results with the terms of equations (1) and (6) to obtain the effective force constant $k_{eff}(x, p) = \mu\omega_E^2(x, p) = 5D_{12}\alpha_{12}^2$ of the effective anharmonic potential. At ambient pressure, the effective force constant is $k_{eff}^0 = 23D_{12}\alpha_{12}^2/4$.

To derive analytical expressions for the cumulants, we use perturbation theory [13, 14]. Atomic vibrations are quantized as phonons, and the phonon–phonon interaction leads to anharmonicity, with the phonon vibration frequency taking the form

$$\omega(x, p) = 2\sqrt{k^0_{eff}/\mu_{12}}\,|\sin(qa_0/2)|, \quad |q \leqslant \pi/a_0|, \quad (7)$$

where a_0 is the lattice constant at temperature T, and q is the phonon wave number. The correlated Einstein frequency and temperature at ambient pressure are respectively

$$\omega^0_{\mathrm{E}} = 2\sqrt{\mathrm{k}^0_{\mathrm{eff}}/\mu_{12}}\,,\ \theta^0_{\mathrm{E}} = \hbar\omega^0_{\mathrm{E}}/\mathrm{k_B}. \quad (8)$$

Using quantum thermodynamic perturbation theory [12] and equations (1), (2), and (8), we obtain the first three EXAFS cumulants as functions of the ambient pressure and temperature. For the first cumulant or net thermal expansion, we have

$$\begin{aligned}\sigma^{(1)}(p, T) &= \sigma^{(1)}_0(p)\frac{(1 + z(p, T))}{(1 - z(p, T))}\\ &= \frac{3\hbar\omega^0_E}{40\mathrm{D}_{12}\alpha_{12}}\frac{(1 + z(p, T))}{(1 - z(p, T))},\\ \sigma^{(1)}_0(p) &= \frac{3\hbar\omega^0_E}{40\mathrm{D}_{12}\alpha_{12}},\end{aligned} \quad (9)$$

for the second cumulant or the DWF we have

$$\begin{aligned}\sigma^{(2)}(p, T) &= \sigma^2_0(p)\frac{(1 + z(p, T))}{(1 - z(p, T))}\\ &= \frac{\hbar\omega^0_E}{10D_{12}\alpha^2_{12}}\frac{(1 + z(p, T))}{(1 - z(p, T))},\\ \sigma^2_0(p) &= \frac{\hbar\omega^0_E}{10D_{12}\alpha^2_{12}},\end{aligned} \quad (10)$$

and for the third cumulant we have

$$\begin{aligned}\sigma^{(3)}(p, T) &= \sigma^{(3)}_0(p)\frac{(1 + 10z(p, T) + (z(p, T))^2)}{(1 - z(p, T))^2}\\ &= \frac{3\hbar^2(\omega^0_E)^2}{200D^2_{12}\alpha^3_{12}}\frac{(1 + 10z(p, T) + (z(p, T))^2)}{(1 - z(p, T))^2},\\ \sigma^{(3)}_0(p) &= \frac{3\hbar^2(\omega^0_E)^2}{200D^2_{12}\alpha^3_{12}}.\end{aligned} \quad (11)$$

We also obtain the thermal expansion coefficient α_{T} and the anharmonic factor β(T, p) as functions of ambient pressure and temperature as

$$\begin{aligned}\alpha(\mathrm{p, T}) &= \alpha_0(\mathrm{p, T})\frac{\mathrm{z(p, T)ln\,(z(p, T))^2}}{(1 - \mathrm{z(p, T))^2}},\\ \alpha_0(\mathrm{p, T}) &= \frac{3\mathrm{k_B}}{20\mathrm{D}_{12}\alpha_{12}\mathrm{r}},\end{aligned} \quad (12)$$

$$\begin{aligned}\beta(p, T) &= \frac{9\eta k_B T}{16\mathrm{D}_{12}}\left[1 + \frac{3k_B T}{8D_{12}R\alpha_{12}}\left(1 + \frac{3k_B T}{8D_{12}R\alpha_{12}}\right)\right],\\ \eta &= \frac{2z(p, T)}{1 + z(p, T)}.\end{aligned} \quad (13)$$

Table 1. Parameters of Morse potential for pure metals and their intermetallic alloy.

Crystal	D_{12}(eV)	$D^{\mathrm{expt.}}_{12}$(eV)	α_{12}(Å^{-1})	$\alpha^{\mathrm{Exp.}}_{12}$(Å^{-1})
Cu-Cu	0.3429	0.3528	1.3588	1.4072
Ag-Ag	0.3323	0.3253	1.3690	1.3535
CuAg72	0.3381	—	1.3634	—

The second cumulant σ^2 contributes to the anharmonic EXAFS amplitude, while $\sigma^{(1)}$ and $\sigma^{(3)}$ contribute to the phase shift of the EXAFS due to anharmonicity. Note that $\sigma^{(1)}$, $\sigma^{(3)}$, and $\alpha(p, T)$ contain the anharmonicity parameter k_{3eff} and exist only when this parameter is included, which is why $\sigma^{(1)}$, $\sigma^{(3)}$, and $\alpha(p, T)$ must be considered when calculating the anharmonic effects in EXAFS. Under ambient pressure, the factor β is proportional to the temperature and inversely proportional to the shell radius, which is consistent with the anharmonicity obtained in experimental research into catalysis [16], and R is considered as the particle radius. In equations (9)–(13), $z(p, T) = \exp(-\theta^0_E/T)$ is the heat and pressure function, which describes how the cumulants, the thermal expansion coefficient, and the anharmonic factor depend on the absolute temperature T and pressure applied to the intermetallic alloy.

3. Results and discussion

For Cu-Cu and Ag-Ag pure metals and the alloy CuAg72, table 1 gives the calculated and experimental [17] parameters of the Morse potential, D_{12} and α_{12}, respectively. Substituting the parameters D_{12} and α_{12} from table 1 into equation (8), with the Boltzmann constant $\mathrm{k_B} = 8.617 \times 10^{-5}\mathrm{eVK^{-1}}$ and Planck's constant $\hbar = 6.5822 \times 10^{-16}$ eV.s, we calculate the values of the Einstein frequency and temperature at ambient pressures up to 14 GPa for Cu-Cu, Ag-Ag, and CuAg72 crystals, and hence deduce the local force constant. Table 2 lists the results, where $\mathrm{k^{expt.}_{eff}}$ is the local force constant deduced from the results of Okube *et al* [18, 19].

Inserting the thermodynamic parameters from tables 1 and 2 into equations (1) and (9)–(13) gives the effective anharmonic potential $\mathrm{V_E(x, p)}$ as a function of the departure x from equilibrium bond length and ambient pressure (see figure 1). The cumulants $\sigma^{(\mathrm{n})}$(n) depends on the absolute temperature T and are influenced by pressure up to 14 GPa (see figures 2–5). Figure 6 shows the thermal expansion coefficient α(T, p) as a function of absolute temperature T and pressure, and figure 7 shows the anharmonic factor β(T, p).

Thermodynamic properties and anharmonic effects of materials depends on the atomic interaction under pressure effect described by the anharmonic interatomic effective potentials V(x) presented in figure 1. Anharmonic interatomic effective potentials V(x) of CuAg72 calculated using the present theory compared to the experimental values [20] and other theories [18, 19]. According to present calculated, the blue solid line describe the anharmonic effective potential for

Table 2. Effective parameters describing anharmonicity.

Crystal	$k_{eff}(eVA^2)$	$k_{eff}^{Expt}(eVA^2)$	$k_{eff}^{0}(eVA^2)$	$\omega_E(10^{13}\,Hz)$	$\omega_E^0(10^{13}\,Hz)$	$\theta_E(K)$	$\theta_E^0(K)$
Cu-Cu	3.1655	3.4931	3.6403	3.0889	4.7710	236	364
Ag-Ag	3.1139	2.9797	3.5810	3.3933	3.6585	176	279
CuAg72	3.1423	—	3.6138	2.6874	4.3623	207	333

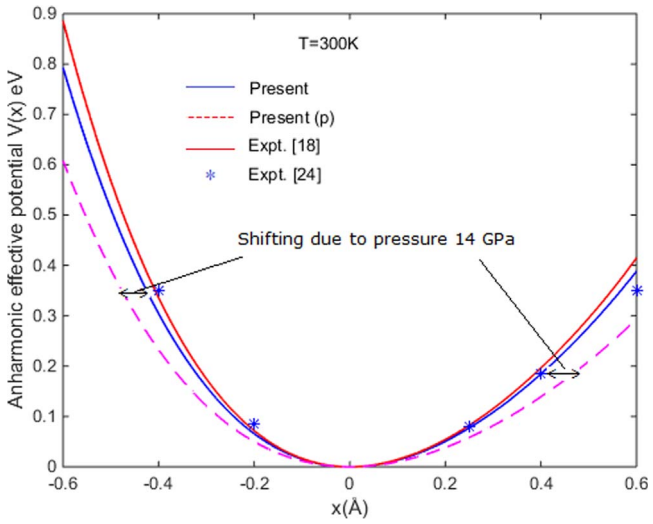

Figure 1. Anharmonic effective potential of CuAg72 (4th order).

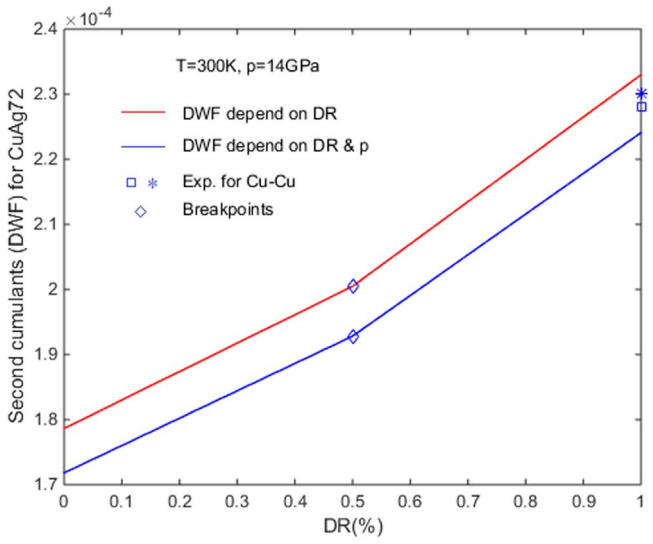

Figure 2. Second cumulant (DWF) depends on doping ratio (DR) and pressure (p) for CuAg72 alloy.

CuAg72 at temperature 300 K, and the dashed curve describe it under the influence of pressure of 14 GPa. The results received align closely with those obtained from the other theories [18, 19] (red solid line), and experimental vulues [20] indicating that the coefficients k_{eff}, k_{3eff}, and k_{eff}^{0} calculated by using the ACEM (given in table 2) are in reasonable agreement with measurements and the calculations of Okube *et al* [19] and experimental results [20].

Figure 2 shows our calculation of the second cumulant or DWF as a function of the doping ratio (DR) at 300 K and an ambient pressure of 14 GPa for the crystalline alloy CuAg72.

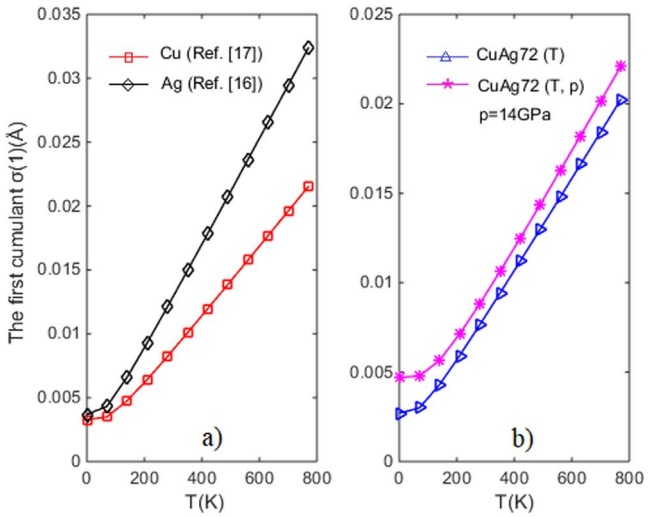

Figure 3. The first cumulant for Cu, Ag, CuAg72.

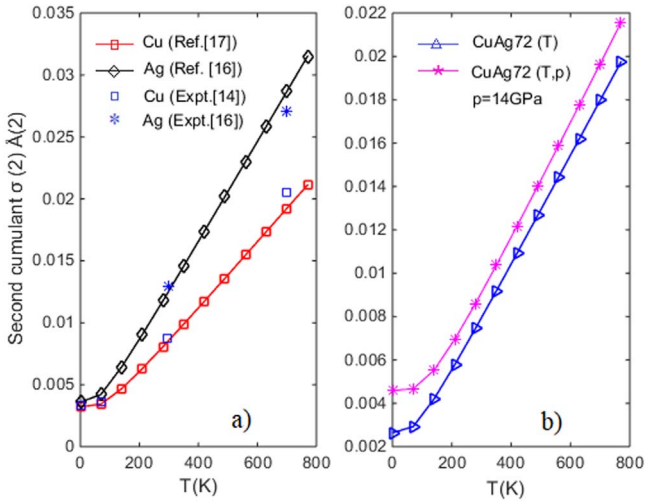

Figure 4. The second cumulant for Cu, Ag, and CuAg72.

These results illustrate that for DRs of 0%–50% and 50%–100%, the DWF varies linearly with the DR (with different slopes in each range). For DR = 100% (i.e., where the Ag content is 0% and the Cu content is 100%) the calculated values are in good agreement with experimental values determined at 300 K (see symbols *, □) [21–23]. However, there are breakpoints in the lines at 50% DR, which means that we do not have ordered atoms at DR = 50%. Thus, the Cu-Ag alloy does not form an ordered phase at the molar composition of 1:1 (i.e., the alloy CuAg50 does not exist), and this result is consistent with the findings of Kraut and Stern [10]. As the ambient pressure increases, the DWF decreases: with 0% Ag, 100% Cu, and 101 kPa (i.e., normal

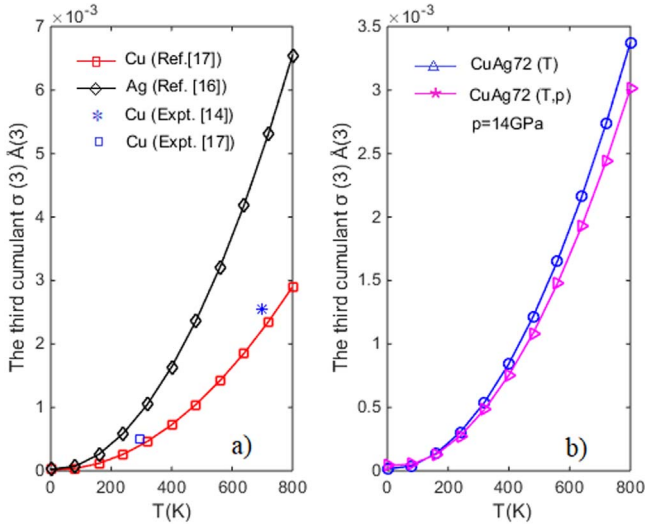

Figure 5. The third cumulant for Cu, Ag, and CuAg72.

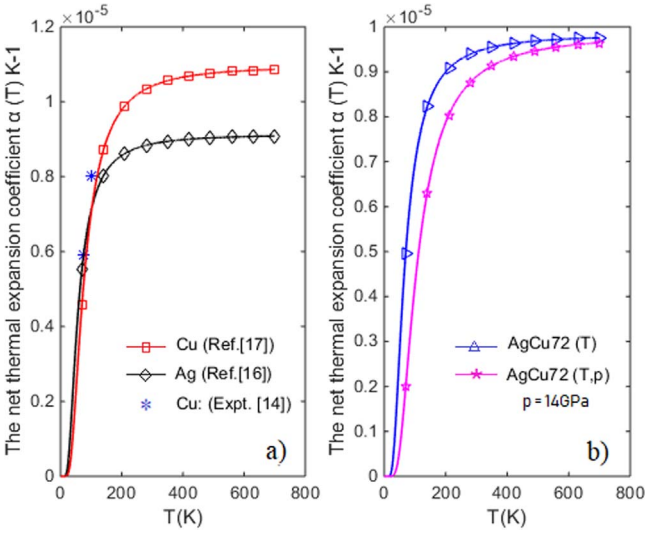

Figure 6. Net thermal expansion coefficient depend T, p.

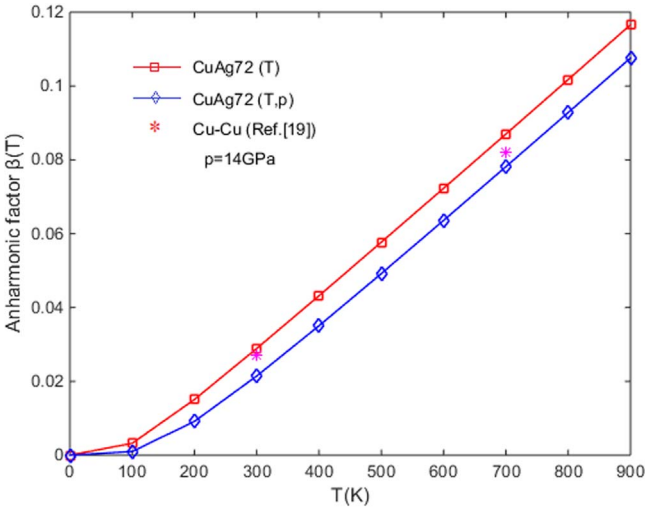

Figure 7. Graph of Anharmonic Factor.

atmospheric pressure), we have DWF = 0.2330 Å^2 (for 14 GPa, DWF = 0.2241 Å^2); with 100% Ag, 0% Cu, and 101 kPa, we have DWF = 0.1796 Å^2 (for 14 GPa, DWF = 0.1718 Å^2). At the breakpoints, we have DWF = 0.2005 Å^2 and 0.1928 Å^2 at 101 kPa and 14 GPa, respectively. Thus, increasing the ambient pressure decreases the EXAFS amplitude by reducing the atomic MSRD that characterizes the EXAFS DWF.

Figure 3 shows the first cumulant $\sigma^{(1)}$ as a function of temperature at the pressure of 14 GPa for Cu, Ag (figure 3(a)), and CuAg72 (figure 3(b)). At approximately the zero point with 101 kPa and 14 GPa ambient pressure, we have $\sigma^{(1)} = 0.0027$ Å and $\sigma^{(1)} = 0.0047$ Å, respectively; at 700 K, we have $\sigma^{(1)} = 0.0184$ Å and $\sigma^{(1)} = 0.0201$ Å, respectively. Thus, as the pressure increases, the first cumulant also increases, but at low temperature it deviates more, meaning that the pressure causing the net thermal expansion is more pronounced at low temperatures.

Figure 4 shows the second cumulant or DWF as a function of absolute temperature with the effects of ambient pressure for Cu-Cu, Ag-Ag (figure 4(a)), and CuAg72 (figure 4(b)) and compares these results with experimental results [21, 22]. The calculated values for the first cumulant (figure 3(b)) and the DWF (figure 4(b)) for different DRs at the pressure of 14 GPa are proportional to temperature from around 100 K and above.

Consider the change in the second cumulant (DWF) for different temperatures. At approximately 0 K, the DWF increases from $\sigma^{(2)} = 0.0026$ Å^2 to $\sigma^{(2)} = 0.0046$ Å^2 as the pressure increases from normal atmospheric pressure up to 14 GPa. At 700 K, the DWF increases from $\sigma^{(2)} = 0.018$ Å^2 to $\sigma^{(2)} = 0.0197$ Å^2 as the pressure increases from normal atmospheric pressure up to 14 GPa. At low temperatures, the DWF changes more than it does at high temperatures because the change in ambient pressure from 101 kPa to 14 GPa causes a greater MSRD of the atoms (or second cumulant $\sigma^{(2)}$). Furthermore, figure 4 shows that from room temperature upward (approximately 300 K), the DWF remains almost constant as the ambient pressure increases, so the ambient pressure has a stronger effect at low temperatures.

Figure 5 shows the third cumulant $\sigma^{(3)}$ for Cu-Cu, Ag-Ag (figure 5(a)), and CuAg72 (figure 5(b)) as a function of absolute temperature and at normal atmospheric pressure (101 kPa) and at the pressure of 14 GPa. The calculated results for Cu-Cu and Ag-Ag are consistent with experimental results [21–23] at normal atmospheric pressure. At 0 K for both 101 kPa and 14 GPa, the third cumulant $\sigma^{(3)} \approx 0$, but as the temperature increases, $\sigma^{(3)}$ for CuAg72 decreases with pressure: at 700 K, we have $\sigma^{(3)} = 0.0026$ Å^3 at 101 kPa and 0.0023 Å^3 at 14 GPa. Thus, high ambient pressure reduces the asymmetry of the atomic interaction potential at higher temperatures.

The results shown in figures 3–5 for CuAg72 at all pressures are very similar to the results for Cu-Cu, demonstrating the consistency between theoretical and experimental results. The calculated first three cumulants contain zero-point contributions at low temperatures, resulting from an asymmetry of the atomic interaction potential due to anharmonicity

even at high pressure, which is consistent with established theories [1, 7, 8, 13].

Figure 6 shows the thermal expansion coefficient α_T for Cu-Cu, Ag-Ag (figure 6(a)), and CuAg72 (figure6b) as a function of absolute temperature with the effects of ambient pressure. The calculated results for Cu-Cu are consistent with experimental results [21] at normal atmospheric pressure; however, the result for CuAg72 is deflected from 70 K^{-1} to 400 K^{-1} when the ambient pressure is 14 GPa, which shows that because of the effect at high pressure, the thermal expansion coefficient α_T for CuAg72 is reduced significantly in the room-temperature range. However, the thermal expansion coefficient for CuAg72 depend of T and CuAg72 depend of T, p changes very little at high pressure when the temperature exceeds 700 K.

The graph of α_T has the form of the specific heat C_V, thus reflecting the fundamental principle of solid-state theory, which states that thermal expansion results from anharmonic effects and is proportional to the specific heat C_V [13, 24]. Our calculated values of α_T approach the constant value α_T^0 at high temperatures and vanish exponentially with θ_E/T at low temperatures, which is consistent with the results of previous research [22–24].

Figure 7 shows the anharmonic factor $\beta(T)$ as a function of absolute temperature and pressure for CuAg72. For both normal and high pressure (14 GPa), $\beta(T)$ is negligibly small at low temperature and increases strongly when the temperature exceeds 100 K. At normal atmospheric pressure, we have $\theta_E = 176$ K for Ag, $\theta_E = 236$ K for Cu, and $\theta_E = 207$ K for CuAg72. At high pressure, we have $\theta_E^0 = 279$ K for Ag, $\theta_E^0 = 364$ K for Cu, and $\theta_E^0 = 333$ K for CuAg72. The results shown in figure 7 are consistent with experimental results [21], which demonstrates that our calculations for CuAg72 are appropriate for normal atmospheric pressure. At temperatures above 100 K with increasing pressure, the anharmonic factor $\beta^0(T)$ is less than at normal pressure $\beta(T)$; in other words, $\beta^0(T) = 0.3125\ \beta(T)$ at 100 K, $\beta^0(T) = 0.7439\ \beta(T)$ at 300 K, and $\beta^0(T) = 0.898\ \beta(T)$ at 700 K. Thus, the anharmonic factor describes the temperature dependence of the anharmonic EXAFS theory under the influence of high ambient pressure.

4. Conclusions

In this work, based on quantum statistical theory and by applying the effective ACEM to EXAFS spectra, we derive analytical expressions for the temperature dependence of the cumulants and thermodynamic parameters of crystalline Cu, Ag, and their alloy CuAg72 under the influence of pressures up to 14 GPa. The expressions for the second cumulant or DWF, the thermodynamic parameters, the effective force constant, and the correlated Einstein frequency and temperature for Cu, Ag, and CuAg72 agree with the known properties for these quantities. The expressions for calculations involving orderly doped crystals have forms similar to those for pure crystals.

Figures 1–7 show the cumulants and thermodynamic parameters for doped crystals as functions of absolute temperature and pressure. The calculated results are consistent with experimental results and other studies of Cu and Ag, and the results for CuAg72 are coherent. Thus, the method developed herein, which is based on applying the ACEM to EXAFS, is appropriate for calculating and analyzing the cumulant and thermodynamic properties of intermetallic alloys.

Acknowledgments

This research is funded by Vietnam National Foundation for Science and Technology Development (NAFOSTED) under grant number 103.01-2019.55.

Conflicts of interest

The authors declare that they have no conflicts of interest.

ORCID iDs

Nguyen Ba Duc https://orcid.org/0000-0001-6190-0588

References

[1] Rehr J J 2000 *Rev. Mod. Phys.* **72** 621
[2] Iwasawa Y, Asakura K and Tada M 2017 *xafs techniques for catalysts nanomaterials and surfaces* (Cham: Springer International Publishing) 9783319438665
[3] Yokoyama T 1999 *J. Synchrotron Radiat.* **6** 323
[4] Hung V V, Hieu H K and Masuda-Jindo K 2010 *Comput. Mater. Sci.* **49** 5214
[5] Bunker G 1983 *Nucl. Instrum. Methods Phys. Res.* **207** 437
[6] Beni G and Platzman P M 1976 *Phys. Rev.* B **14** 1514
[7] Frenkel A I and Rehr J J 1993 *Phys. Rev.* B **48** 585
[8] Hung N V and Rehr J J 1997 *Phys. Rev.* B **56** 43
[9] Nafi A, Cheikh M and Mercier O 2013 *J. Adhes. Sci. Technol.* **27** 2705
[10] Kraut J C and Stern W B 2000 *J. Gold Bulletin* **33** 52
[11] Duc N B, Tho V Q, Hung N V, Khoa D Q and Hieu H K 2017 *Vacuum* **145** 272
[12] Hung N V, Trung N B and Duc N B 2015 *J. Mat. Sci. Appl.* **1** 91
[13] Duc N B, Hieu H K, Binh N T and Nguyen K C 2018 *Sci. & Tech.* (Hanoi: Pub. House)
[14] Hung N V 2014 *J. Phys. Soc. Jpn.* **83** 024802
[15] Tranquada J M and Ingalls R 1997 *Phys. Rev.* B **28** 3520
[16] Clausen B S, Grabæk L, Topsoe H, Hansen L B, Stoltze P, Norskǿv J K and Nielsen O H 1993 *J. Catal.* **141** 368
[17] Benassi E 2018 *Chem. Phys.* **515** 323
[18] Okube M and Yoshiasa A 2001 *J. Synchrotron Radiat.* **8** 937
[19] Okube M, Yoshiasa A, Ohtaka O and Katayama Y 2003 *High Press. Res.* **23** 247
[20] Priog V, Nedoseikina T I, Zarubin A I and Shuraev A T 2002 *J. Phys. Condens. Matter* **14** 1825–32
[21] Hung N V, Duc N B and Frahm R R 2002 *J. Phys. Soc. Jpn.* **72** 1254

[22] Hung N V and Duc N B 1999 *Proc. of the Third Int. Workshop on Material Science* IWOM'S99
[23] Hung N V and Duc N B 2000 *Commun. Phys.* **10** 15
[24] Mir S A, Yousuf S and Gupta D C 2019 *Materials Science and Engineering:* B **250** 114434